The Influence of Nucleation Density and Cooling Rate on Crystallization of Polyethylene from the Melt

G. V. FRASER, A. KELLER, and J. A. ODELL, *H. H. Wills Physics Laboratory, University of Bristol, Royal Fort, Bristol BS8 1TL, England*

Synopsis

Different samples of high-density polyethylene provided different nucleation densities which were assessed by optical microscopy and light scattering. Crystallizations were carried out under controlled cooling rates using a microscope hot stage and DSC from which crystallization temperatures were obtained. It is shown that the effective crystallization temperature is a function of the nucleation density, and a quantitative fit is found with theoretical predictions based on crystallization kinetics. The melting point was, in turn, found to be dependent on nucleation density, through the agency of lamellar thickness as assessed by low-frequency Raman spectroscopy. The effect of cooling rate on melting point is also explained in terms of variation of supercooling. The implications of these effects together with considerations of surface and interior nucleation and sample size are discussed for the industrial processing of polyethylene.

INTRODUCTION

The origin of this paper has been the observation that some commercially available polyethylenes with nominally identical molecular weights had significantly different melting points after they had been crystallized by cooling from the melt at identical rates. It was noticed further that the same samples possessed widely varying spherulitic textures. The samples with the higher melting points had finer textures, which reflects a larger number of spherulite nuclei. For polypropylene, Beck and Ledbetter[1] report the dependence of crystallization temperature upon concentration of nucleating agent and a corresponding effect on physical properties. These observations focused our attention on the possibility of a correlation between the lamellar thickness, which will influence the melting behavior, and the initial nucleation density in materials that have solidified during cooling. The crystallization under consideration is therefore nonisothermal which, as is well known, is the case with mostly all technologically processed material.

To recapitulate the basic theoretical background: nucleation and subsequent crystal growth lead to the formation of chain-folded lamellar crystals which grow out radially in the form of spherulites. The growth rate G of spherulites is well known to be a function of the supercooling ΔT, theoretically predicted, for moderate supercoolings, to take the form[4]

$$G = G_0 e \frac{-C}{T\,\Delta T} \tag{1}$$

C and G_0 are constants and T is temperature (°K). The thickness of lamellar crystals is governed by the crystallization temperatures T_c or, more correctly,

Journal of Applied Polymer Science, Vol. 22, 2979–2989 (1978)

0021-8995/78/0022-2979$01.00

by the supercooling ΔT, where $\Delta T = T_m^0 - T_c$ and T_m^0 is the equilibrium melting point. Theoretical treatments[3,4] show that the lamellar thickness L is related to the supercooling ΔT by

$$L = \frac{2\delta_e T_m^0}{\Delta H_f \, \Delta T} + \delta l \tag{2}$$

where δ_e is the fold surface free energy, ΔH_f is the heat of fusion, and δl is a quantity which varies slowly with supercooling and is a consequence of kinetic theory.[4] In terms of the melting point T_m, we can express this as

$$T_m = T_m^0 \left[1 - \frac{2\delta_e}{\Delta H_f L} \right] \tag{3}$$

On cooling, polymers crystallize over a range of supercoolings; but at any specific temperature, these equations apply, and we shall use these ideas to explain the relationship between nucleation density and supercooling and the consequent effect upon melting point.

EXPERIMENTAL

Because we wished to explore differences in crystallization behavior due to nucleation effects, samples were chosen so as to be similar in other respects. Seven samples, which we have labeled P, Q, R, S, T, U, and V, were selected from batches of Rigidex, Carlona, Unifes, and Elfex commercial polyethylenes so as to have similar melt-flow indices. These materials were all of the extrusion-grade type and, as shown in Table I, possessed similar molecular weight distributions as assessed by GPC. Although there is some variation in molecular weight across the samples, this did not appear to alter the general trends in crystallization behavior observed due to variations in spherulite size. The table also shows some additional information provided by trade literature. Information on possible additives and fortuitous catalyst residues was not available.

For a quick determination of nucleation densities specimens were cooled at the same rate in a Metler hot stage, and their solidification was observed directly through an optical microscope. Comparison of the textures then gave an immediate impression of the relative numbers of spherulites in the different samples enabling them to be placed approximately in order of nucleation densities. When a single specimen was subjected to cycles of melting and recrystallization, the

TABLE I
Properties of the Linear Polyethylenes Used in This Study

	From present work			
	Molecular weight by GPC, $\times 10^{-3}$		As given by manufacturer	
Sample	M_w	M_n	Density, g/cc	Melt flow index
P	61	10.0	0.965	5
Q	62	10.0	0.960	5
R	39	10.0	0.967	4.5
S	46	7.9	0.960	6
T	71	10.0	0.970	6
U	66	12.5	0.970	6
V	66	20.2	0.960	5

number and spatial arrangement of the spherulites were essentially constant which confirmed the heterogeneous origin of the nucleation in these experiments.

We have two comments to make regarding observations using the optical microscope. Firstly, in some cases appreciable surface nucleation was observed in the thin films. This effect was quite remarkable in sample V, which is discussed in detail later in this paper. Secondly, although it was possible by direct observation to see characteristic differences in textures in the case of the finest and coarsest spherulites, it was not always possible to place intermediate samples in order of spherulite sizes. Thus, at a later stage a quantitative assessment of spherulite size was made using low-angle scattering of laser light by thin sections cut from blocks of the samples. Samples for this purpose were prepared by cooling from the melt in a suitable mold at a rate of 4°C/min. Sections ~40 μ thick and 0.3 cm in diameter were cut using a sledge microtome.

Our scattering apparatus consisted of a helium–neon laser operating at 1 m W to illuminate a specimen held between microscope cover slips. The diameter of the laser beam was adjusted so as to sample as large a proportion of the sample as possible. A specimen-to-film distance of 40 cm was used. The scattered light passed through an analyzer and was recorded on photographic film. The method relies on the anisotropic scattering of polarized light by the spherulites to produce, in the case where the polarization direction of the analyzer is perpendicular to that of the laser, the H_v configuration, a four-leaf clover pattern.[5] The intensity distribution of pairs of opposite lobes was scanned using a densitometer, and a value of the distance from the center of the pattern to the lobe maximum was obtained. This enabled the scattering angle corresponding to the lobe maximum θ_m to be found. The spherulite size was calculated from θ_m using the relationship[5]

$$R = \frac{\lambda}{\pi \sin(\theta_m/2)}$$

where λ = wavelength of incident light, which was 632.8 nm in our experiments. Surface irregularities on the films scramble the polarization of the incident beam and lead to intense uniform background scattering. In order to reduce this, the specimens were placed in a contact fluid between the cover slips. The most convenient fluid available was a microscope immersion fluid of refractive index 1.59. In addition to this effect, the finest textured samples gave a diffuse pattern in which the lobes were not as well defined as in the patterns of the coarser-textured samples. For the fine textures, more than one spherulite may be accommodated within the thickness of the film. This diffuse scatter may therefore have arisen from secondary scattering at spherulite boundaries. The spherulite sizes obtained from the light-scattering experiments confirmed the trends observed using optical microscopy.

Lamellar thicknesses were determined using low-frequency Raman spectroscopy. Unlike the low-angle scattering of light used to measure spherulite size, Raman spectroscopy utilizes an inelastic scattering effect.[6] Monochromatic laser light is scattered by a specimen at discrete frequencies corresponding to molecular vibrations. One of these vibrations is the longitudinal acoustical mode, or LAM, whose frequency is inversely proportional to the length of the vibrating chain. In crystalline polyethylene, the LAM frequency is related to the length of the chains between the fold surfaces of the lamellae and is therefore a measure

of the lamellar thickness. This method of measuring lamellar thickness was first exploited for a polymer by Peticolas et al.[7] and has since been developed by a number of workers.[8–10] The Raman lamellar thickness was calculated using the relationship

$$L = \frac{m}{2\nu}\left[\frac{E}{\rho}\right]^{1/2}$$

where E = Young's modulus of the chain = 3.4×10^{12} dynes/cm^2, ρ = crystalline density = 0.997, m = mode order = 1, and ν is the molecular vibrational frequency. The LAM occurs at frequency shifts close to that of the exciting radiation and therefore requires a spectrometer with excellent stray light at low-frequency shifts. We used a Coderg T800 Raman spectrometer and a krypton ion laser operated at 530.9 nm to excite the spectra. Raman spectroscopy was used in preference to small-angle x-ray diffraction for these experiments because of the short time required (~10 min) to obtain each value of lamellar thickness.

For a detailed examination of the range of supercooling over which the specimens crystallized, a Perkin-Elmer DSC 1B was used. The following routine was employed: Specimens of each sample were cooled from the melt at known cooling rates to room temperature. The temperature corresponding to the exotherm peak was taken as the crystallization temperature for defining the effective supercooling ΔT^e. Each specimen was removed from the DSC pan and examined by Raman spectroscopy to determine the lamellar thickness. Then, the sample was returned to the DSC and its melting point was determined. There is a limit to the cooling rate a specimen of a given thickness can follow. Beyond this thickness the cooling rate is governed by diffusion of heat through the specimen. In this situation the melting points of slowly reheated specimens no longer show any correlation with the apparent T_c. In practice, this can be avoided by using sufficiently thin specimens.

RESULTS

Figure 1 shows the different spherulite sizes obtained to illustrate the starting point of our observations. The order of the spherulite sizes in the different samples of polyethylene is shown in Table II. A selection of cooling rates was used ranging from 0.2° to 10°C/min, which are the limits of the microscope hot stage. Any sample of the same material gave the same spherulite size under identical crystallization conditions. Little variation in texture was observed for the same sample over this range of cooling rates. The effect persisted when specimens were heated up to 250°C to ensure that all memory of the solid structure had been destroyed. Each grade, therefore, possesses a characteristic spherulitic texture. It can be seen that the spherulite sizes as determined by light scattering are in the range of 9–29 μ, with the exception of material V, whose spherulites are much larger, in fact, the spherulite size depended upon the cooling rate employed during crystallization. Rapid cooling gave large spherulites (~80 μ in diameter), while slow cooling or isothermal crystallization at high temperatures (120°C) produced a fine texture on a similar scale to that observed for samples P to U.

Further investigation revealed that the fine structure in sample V is due to crystallization nucleated by the glass surfaces which contain the polymer. This

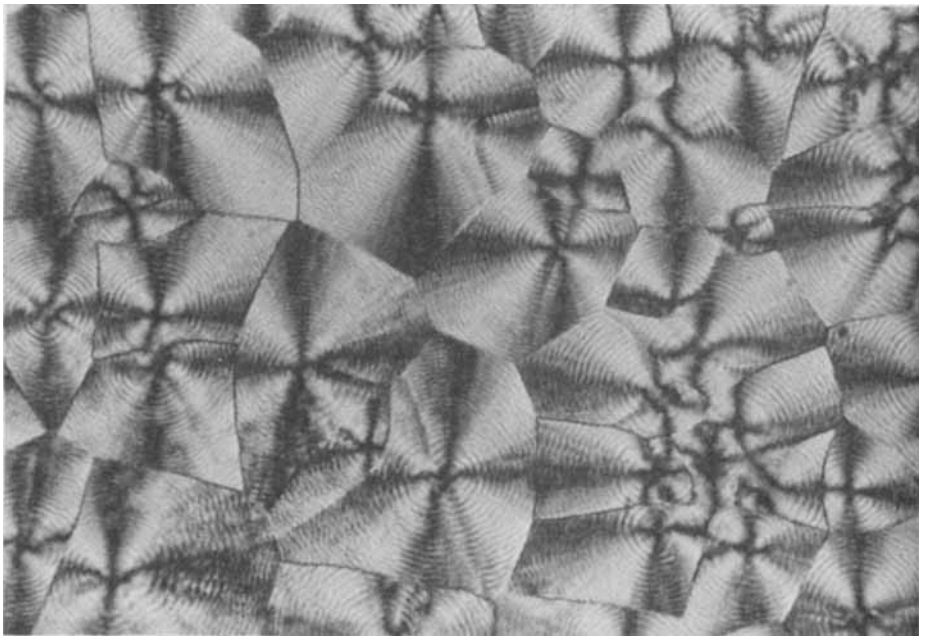

(a)

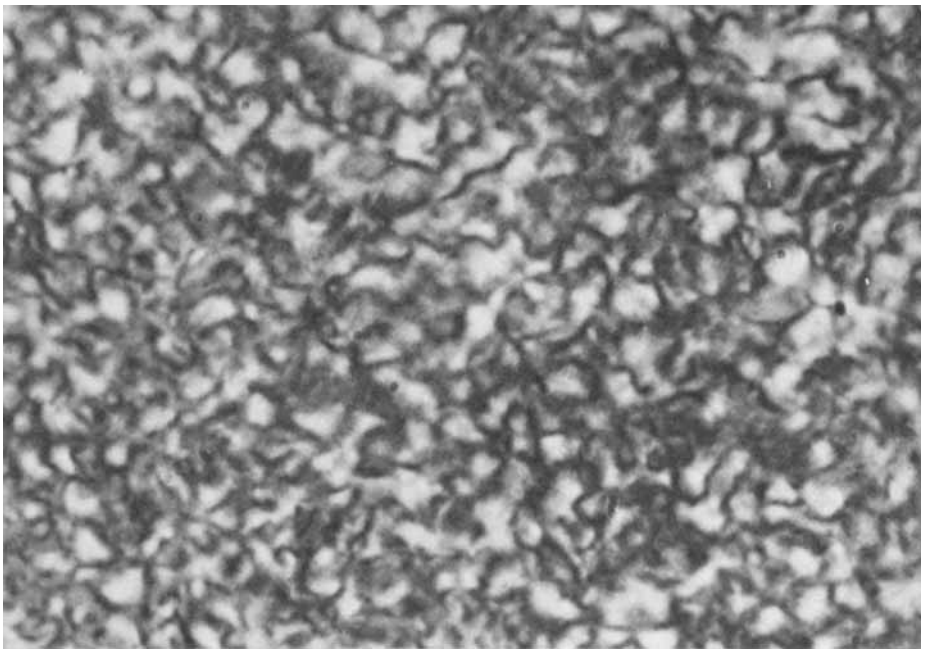

(b)

Fig. 1. Micrographs of spherulites with different textures: (a) large spherulites in sample V, ~80 μ; (b) small spherulites in sample S, ~21 μ; and (c) surface nucleation effects in sample V.

produces a region of transcrystallized material which overlays the heterogeneously nucleated material and makes the structure appear much finer. A section through such a polymer sample is shown in Figure 1(c). These surface

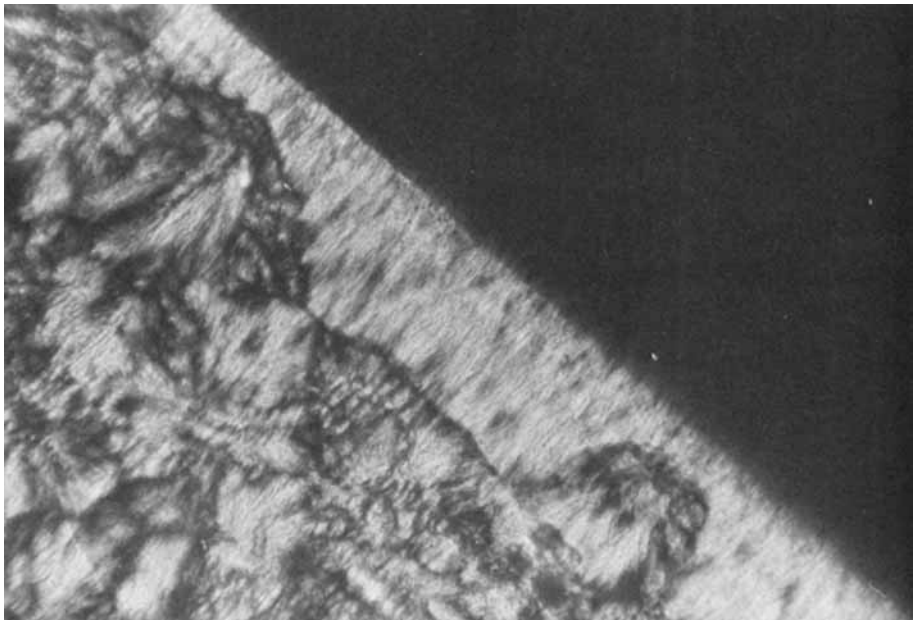

(c)
Fig. 1 (Continued from previous page).

nuclei become active at a higher temperature than the internal nuclei; slow cooling permits considerable surface crystallization, while rapid cooling results in nucleation behavior dominated by the interior nuclei. Surface nucleation had only a very small effect in samples P to U due to the greater effectiveness of their internal nuclei at high crystallization temperatures. The following studies were therefore confined to samples P to U.

Figure 2 shows the spherulite size plotted against the effective supercooling ΔT^e ($\Delta T^e = T_m^0 - T_c^e$, where $T_m^0 = 145°C$). It can be seen that samples with a high nucleation density crystallized at a lower supercooling than samples with a low nucleation density. There is a nearly linear relationship between final spherulite size and ΔT^e. It will be clear that by affecting the supercooling at which crystallization occurs the nucleation density will also affect the lamellar thickness. This is shown by the measurements in Figure 3. It is to be expected that the lamellar thickness in turn should influence the melting points of the resulting crystals as in fact observed and shown in Figure 4. In both respects (Figs. 3 and 4) there is again a strong correlation with spherulite size. The experimental points in Figure 5 show the effect of cooling rate on T_c for sample S only (21-μ spherulites).

TABLE II
Spherulite Sizes of Linear Polyethylenes Crystallized by Cooling from the Melt at 4°C/M

Sample	P	Q	R	S	T	U	V
Size, μ	9	13	18	21	26	29	80

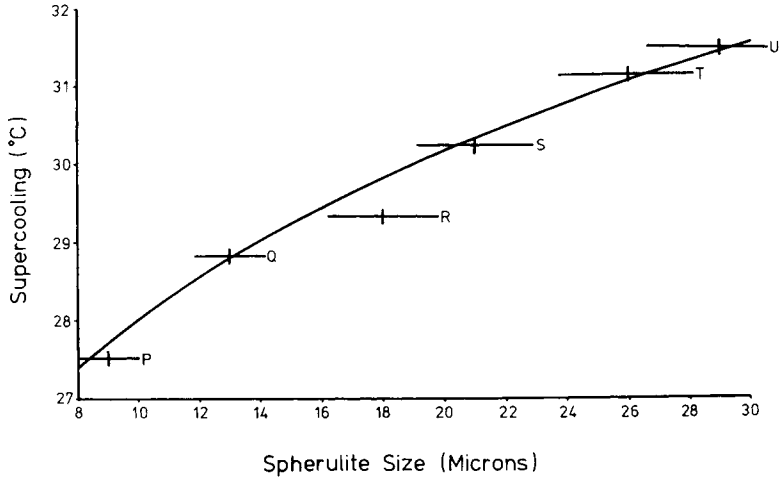

Fig. 2. Experimental correlation between spherulite size and supercooling (effective, ΔT^e), together with a theoretical curve derived as explained in the text for identical cooling rates.

DISCUSSION

When a material is crystallized at a set cooling rate, the supercooling increases in proportion to elapsed time. For a cooling rate ρ, the growth rate as a function of elapsed time t becomes

$$G = G_0 \exp\left[-\frac{C}{\rho t(T_m - \rho t)}\right] \tag{4}$$

The general form of this equation is shown in Figure 6 (G_0 and C are constants).

Generally, the rate of crystallization increases with the linear rate of growth until the growing spherulites begin to impinge upon one another, after which the rate of crystallization must fall rapidly due to the reduction in growth front

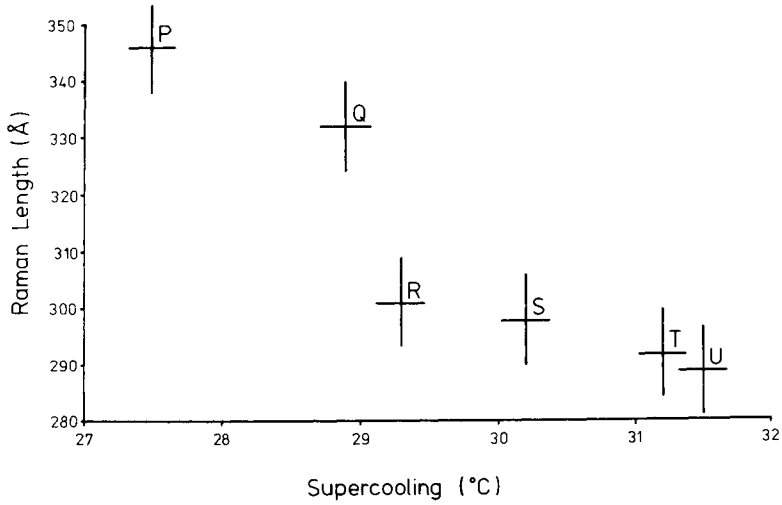

Fig. 3. Experimental correlation between Raman lamellar thickness L_R and supercooling (ΔT^e).

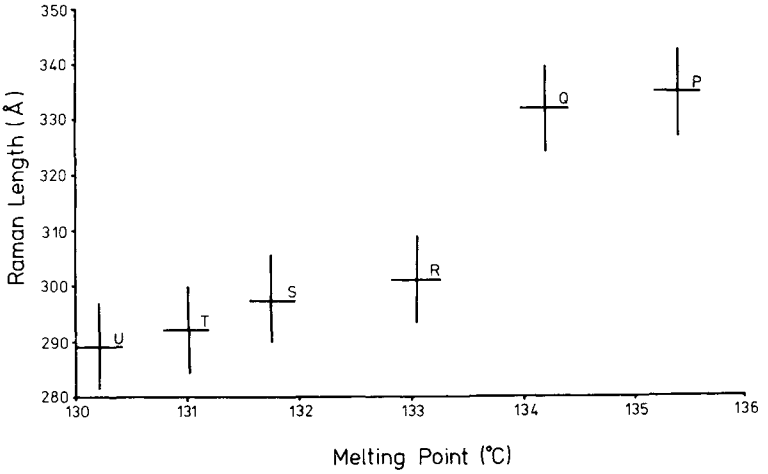

Fig. 4. Experimental correlation between Raman lamellar thickness L_R and melting point (T_m).

(although the radial growth rate will continue to increase). This maximum rate of crystallization corresponds to the peak of DSC curves of crystallization.

The time required for a set number of the growing spherulites to reach the point of impingement can be predicted by integration of the growth rate with respect to the time to obtain the size of the growing spherulite as a function of time.

The form of eq. (4) is such that analytical integration is not possible. However, a knowledge of the constants G_0 and C would enable numerical integration and hence prediction of the supercooling as a function of final spherulite size. The unexpected good experimental correlation between final spherulite size and supercooling leads us to enquire whether the results could be explained on this basis. The following trial-and-error procedure was adopted. Values of the constants G_0 and C were varied until a good fit was found with the experimental data. Figure 2 shows a curve derived in this way, which superimposes well upon

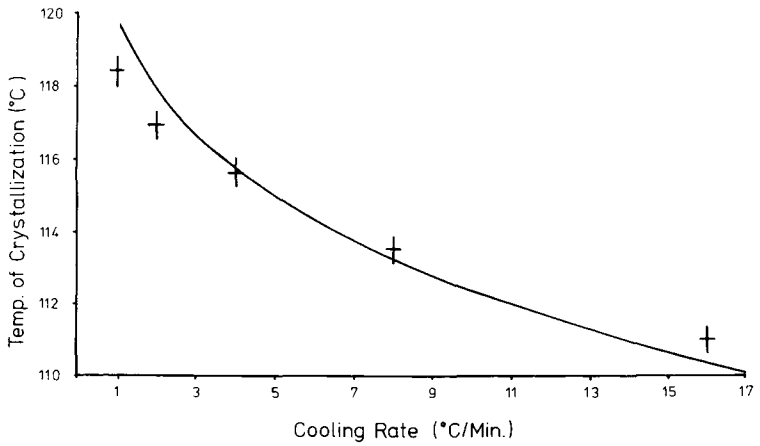

Fig. 5. Correlation between cooling rate and crystallization temperature T_c^s (temperature at which the crystallization rate is fastest) for sample S: (+) experimental points (DSC peak positions); (−) theoretical curve.

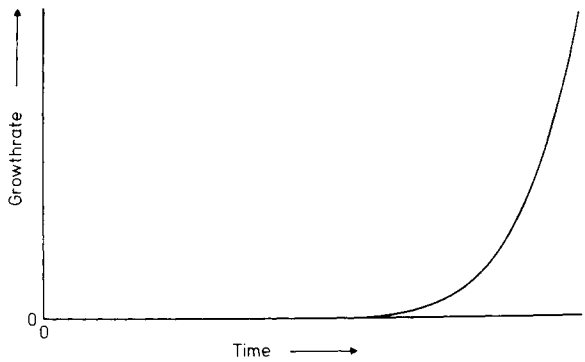

Fig. 6. Schematic diagram of the relationship between spherulite growth rate G and elapsed time t during cooling from the melt on a set rate ρ.

the experimental points. The values of the growth rate parameters which were used to generate this curve are $G_0 = 5.65 \times 10^2\ \mu\ \text{sec}^{-1}$ and $C = 9.3 \times 10^4$. These agree well with previously reported values,[11,12] which are in the range of (3–11) $\times 10^2\ \mu\ \text{sec}^{-1}$ for G_0 and (7–9) $\times 10^4$ for C (after due correction has been made for the different values adpoted for T_m^0 by various authors). It should be pointed out, however, that the works quoted were confined almost entirely to the crystallization of narrow molecular weight fractions, whereas we have used disperse commercial polyethylenes. However, the quantitative aspects are not so important here. Rather, we wish to emphasize that there is a basis in theory for the observed correlation between ΔT^e and final spherulite size. Nevertheless, our results for samples with similar molecular weight distributions indicate similar growth rate constants.

From eq. (2) relating lamellar thickness and supercooling, we can see that a sample which crystallizes at low supercooling should have lamellae whose thickness is larger than in a sample that crystallizes at an average higher supercooling. Accordingly, as shown in Figure 3, we observe that samples which crystallized at low supercooling are those with thick lamellae; and by comparison with Table II we see that these are the samples with the highest nucleation densities. Thus, we can see immediately that the number of nuclei determines the thickness of the lamellar units of which the superulites are composed. This is in addition to the commonly known fact that the nucleation density determines the size of the spherulites.

The effect of nucleation density on the melting point follows as a natural consequence from the control of lamellar thickness by the nucleation density. We observe experimentally that the higher melting points belong to the samples with the higher nucleation densities. In the previous discussion, we established that the higher nucleation densities resulted in crystallization at a higher temperature and hence thicker lamellae. The correlation between thicknesses and melting point is given in Figure 4, from which we see that the thicker lamellae melt at higher temperatures. This is in accordance with eq. (2), in which the melting point is inversely proportional to the lamellar thickness. The original observation of a connection between spherulite size and melting point is thus explained.

In an earlier paper[10] we noted that the nucleation density influenced the process of lamellar thickening when crystallizations were carried out isothermally.

This is of interest here since the effect of nucleation density during cooling is to determine the amount of material available for thickening at any specific supercooling. In the case of isothermal crystallization, the materials with the highest nucleation densities had on average the oldest and hence the thickest lamellae at any given stage during the crystallization process. Clearly, this process must also operate during crystallization from the melt by cooling. However, at the cooling rates used in this study, the crystallization time is too short to permit lamellar thickening to have a significant effect.

The cooling rate employed during crystallization dramatically affects the crystallization temperature and hence the lamellar thickness. Qualitatively, it is clear that faster cooling enables the achievement of higher supercooling before spherulite impingement.

Numerical integration of eq. (4) enables the calculation of spherulite size as a function of both elapsed time and cooling rate. Thus, for a specific distance between spherulite centers the time required for the spherulites to impinge (and hence the corresponding supercooling ΔT^e) can be calculated as a function of cooling rate. As mentioned earlier, the point of spherulite impingement should closely correspond with the observation of maximum rate of crystallization by DSC.

This calculation has been performed for material S, which has a mean spherulite size of 21 μ. The values of G_0 and C were those derived earlier. The solid line of Figure 5 shows the results for cooling rates between 1° and 16°C/min. Also shown in Figure 5 are experimental measurements of T_c^e for different cooling rates from DSC measurements. Here again, the correspondence between theory and experiment is good. A corresponding dependence of lamellar thickness and melting point on cooling rate has been observed.

All the above correspondences applied to materials P to U. Material V was not represented. While interesting in its own right by virtue of the large spherulites it produces, its behavior did not conform with the rest of the series. It needs noting at this juncture that the assumption implicit in all the previous considerations was that the spherulite growth rates are identical and so is their variation with temperature in the different source materials. The quantitative fit for the six materials P to U confirms that this assumption applies. In fact, the identity of spherulite growth rates in materials of different origin can be regarded as one salient conclusion of the work. Conversely, the fact that sample V does not fit into the picture suggests that this identity of growth rate does not hold. Here, we do not attempt to unravel the reasons for the anomaly in this material. However, it is possible that this effect is produced by additives contained by this particular material over which we have had no control.

CONCLUSIONS

We have demonstrated how the nucleation density influences not only the scale of the spherulite texture in polyethylene solidified during cooling, but also the properties of the lamellar crystals of which the spherulites are composed. During cooling, the distance between spherulite nuclei determines the supercooling at which the spherulites impinge. This, in turn, controls the effective temperature of crystallization and hence the lamellar thickness. This can fully account for the observed effect of nucleation density and cooling rate on the melting point of polyethylene. If the density of internal nuclei is very low, then competitive surface nucleation occurs.

The effects of nucleation density are of consequence for the industrial processing of polyethylene during cooling, and it is hoped that the present study provides some guides to their interdependence and possible control.

The authors wish to thank the following for their assistance: Dr. P. Volans of Monsanto for supplying samples, A. Halter for determining molecular weight distributions under the guidance of Dr. J. Stejny, and Dr. P. L. Goggin for providing spectroscopic facilities. J. A. O. wishes to acknowledge the Ministry of Defence and I. C. I. and G. V. F., the Science Research Council for financial support.

References

1. H. N. Beck and H. D. Ledbetter, *J. Appl. Polym. Sci.*, **9,** 2131 (1965).
2. P. H. Lindenmeyer and V. F. Holland, *J. Appl. Phys.*, **35,** 55 (1964).
3. F. C. Frank and N. Tosi, *Proc. R. Soc.*, **A263,** 323 (1961).
4. J. D. Hoffman and J. I. Lauritzen, *J. Appl. Phys.*, **44,** 4340 (1973).
5. R. S. Stein and M. B. Rhodes, *J. Appl. Phys.*, **31,** 1873 (1960).
6. G. Herzberg, *Infrared and Raman Spectra of Polyatomic Molecules,* Van Nostrand, New York, 1945.
7. W. L. Peticolas, G. W. Hibler, J. L. Lippert, A. Peterlin, and H. Olf, *Appl. Phys. Lett.*, **18,** 87 (1971).
8. P. J. Hendra, H. P. Jobic, and K. Holland-Moritz, *Polym. Lett.*, **13,** 365 (1975).
9. S. L. Hsu and S. Krimm, *J. Appl. Phys.*, **47,** 4265 (1976).
10. J. Dlugosz, G. V. Fraser, D. Grubb, A. Keller, J. A. Odell, and P. L. Goggin, *Polymer,* **17,** 471 (1976).
11. W. Banks, J. N. Hay, A. Sharples, and G. Thompson, *Polymer,* **5,** 163 (1964).
12. I. Heber, *J. Polym. Sci.*, **A2,** 1291 (1964).

Received April 13, 1977
Revised July 15, 1977